

Eruptive history of a low-frequency and low-output rate Pleistocene volcano, Ciomadul, South Harghita Mts., Romania

Alexandru Szakács · Ioan Seghedi · Zoltán Pécskay · Viorel Mirea

Received: 25 February 2014 / Accepted: 9 December 2014
© Springer-Verlag Berlin Heidelberg 2015

Abstract Based on a new set of K–Ar age data and detailed field observations, the eruptive history of the youngest volcano in the whole Carpathian-Pannonian region was reconstructed. Ciomadul volcano is a dacitic dome complex located at the southeastern end of the Călimani-Gurghiu-Harghita Neogene volcanic range in the East Carpathians. It consists of a central group of extrusive domes (the Ciomadul Mare and Haramul Mare dome clusters and the Köves Ponk dome) surrounded by a number of isolated peripheral domes, some of them strongly eroded (Bálványos, Puturosul), and others topographically well preserved (Haramul Mic, Dealul Mare). One of the domes (Dealul Cetății) still preserves part of its original breccia envelope. A large number of bread-crust bombs found mostly along the southern slopes of the volcano suggest that the dome-building activity at Ciomadul was punctuated by short Vulcanian-type explosive events. Two late-stage explosive events that ended the volcanic activity of Ciomadul left behind two topographically well-preserved craters disrupting the central group of domes: the larger-diameter, shallower, and older Mohoș phreatomagmatic crater and the smaller, deeper and younger Sf. Ana (sub)Plinian crater. Phreatomagmatic products of the Mohoș center, including accretionary lapilli-bearing base-surge deposits and poorly sorted airfall deposits with impact sags, are known close to the eastern crater rim. A

key section studied in detail south of Băile Tușnad shows the temporal succession of eruptive episodes related to the Sf. Ana (sub)Plinian event, as well as relationships with the older dome-building stages. The age of this last eruptive event is loosely constrained by radiocarbon dating of charcoal pieces and paleosoil organic matter at ca. 27–35 ka. The age of the Mohoș eruption is not constrained, but we suggest that it is closely related to the Sf. Ana eruption. The whole volcanic history of Ciomadul spans over ca. 1 Myr, starting with the building up of peripheral domes and then concentrating in its central part. Ciomadul appears as a small-volume (ca. 8.74 km³) and very low-frequency and low-output rate volcano (ca. 9 km³/Myr) at the terminus of a gradually diminishing and extinguishing volcanic range. A number of geodynamically active features strongly suggest that the magma plumbing system beneath Ciomadul is not completely frozen, so future activity cannot be ruled out.

Keywords Pleistocene volcanism · East Carpathians · Ciomadul · Dacite dome complex · Phreatomagmatic craters · Volcanic evolution · Radiometric ages

Editorial responsibility: P. Wallace

A. Szakács (✉)
Department of Environmental Sciences, Sapientia University,
Cluj-Napoca, Romania
e-mail: szakacs@sapientia.ro

A. Szakács · I. Seghedi · V. Mirea
Romanian Academy, Institute of Geodynamics, Bucharest, Romania

Z. Pécskay
Hungarian Academy of Science, Institute of Nuclear Research
(ATOMKI), Debrecen, Hungary

Introduction

Volcanic domes, also called lava domes, are common features in active and ancient volcanic areas worldwide, in particular where viscous magma (with compositions from andesitic to rhyolitic) erupts (Fink and Anderson 2000). They occur either as parts of larger composite volcanic edifices or as isolated or clustered formations (i.e., dome complexes). Their eruption mechanisms, typology and characteristic features were reviewed by Fink and Anderson (2000), while their role in

generating geothermal features is discussed extensively by Wohletz and Heiken (1992). What we currently know about lava dome eruption mechanisms is based on observation of active volcanoes (Fink and Anderson 2000) such as Mount St Helens (USA.) (e.g., Scott et al. 2008), Colima (Mexico) (e.g., Luhr 2002), Soufriere Hills (Montserrat) (e.g., Clarke et al. 2007), and Santiaguito (Guatemala) (e.g., Scott 2013). In all these cases, dome-building activity was related to existing composite volcanoes. Domes and dome complexes are also found in both early and late stages of silicic caldera evolution as well as along major tectonic lineaments such as grabens and rifts (Wohletz and Heiken 1992). Isolated volcanic domes and dome complexes, not related to larger edifices such as calderas or composite volcanoes, are poorly known.

Small-volume, yet long-lived (1 Myr or more) volcanoes with eruptive histories consisting of very low-frequency events are among the less well-studied and understood volcanoes on Earth. Ciomadul volcano in the South Harghita Mts., Romania (Fig. 1), a dacitic dome complex, is one of them. The particular interest in this volcano arises from the fact that it is part of a trend in the evolution of the Călimani-Gurghiu-Harghita volcanic range in the East Carpathians from NW to SE along the range: gradually smaller-volume volcanic edifices, decreasing magma production volumes and output rates (Szakács et al. 1997) and changes in magma compositions from normal calc-alkaline to high-K calc-alkaline to shoshonitic (Szakács et al. 1993). The internal structure of volcanic edifices also changed from typical large-volume stratovolcanoes (two of them caldera-forming) to smaller-volume composite volcanoes (with early-stage stratovolcano-type edifices topped with dome complexes) to even smaller-volume dome complexes and, finally, monogenetic constructs (Szakács and Seghedi 1995).

Furthermore, of the ca. 21-Myr-long volcanic history within the broader Carpathian-Pannonian Region (CPR) (Pécskay et al. 2006), the most recent manifestations of volcanic activity at Ciomadul are of particular interest not only for their very young age but also because any discussion addressing the issue of possible volcanic hazard from sources located within CPR starts with reference to the most recent eruptions (Szakács and Seghedi 2013). Too, up-to-date information is due to be incorporated in a worldwide database concerning Quaternary global volcanic activity, currently being undertaken (Crosweller et al. 2012).

This contribution focuses on revealing the volcanic structure and evolution of Ciomadul volcano on the basis of all previously published data and new geological and geochronological information. As a consequence, the chronology of major eruptive events and the development of volcanic structures for a rare, long-lived, low eruption-frequency volcano are now better understood.

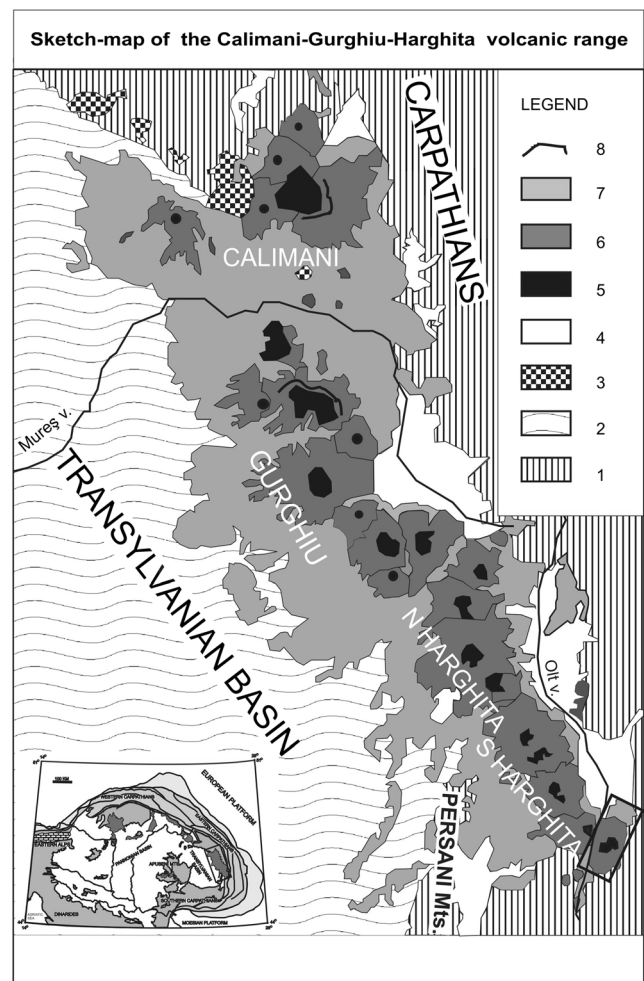


Fig. 1 Location of Ciomadul volcano (framed) within the Călimani-Gurghiu-Harghita volcanic range (after Szakács and Seghedi 1995, modified). Legend: 1, East Carpathians fold-and-thrust range; 2, Transylvanian Basin; 3, intrusive magmatic bodies of the “Subvolcanic Zone”; 4, Pliocene-Quaternary intramountain basins; 5–8, volcanic facies of Neogene volcanic edifices; 5, central facies; 6, proximal facies; 7, medial/distal facies; 8, topographic caldera-crater rim. *Inset* shows the location of the Călimani-Gurghiu-Harghita volcanic range within the Carpathian-Pannonian Region (Europe)

Regional setting

Ciomadul is the main chain-ending volcano in the South Harghita Mts., which is the southern segment of the Călimani-Gurghiu-Harghita volcanic range (CGH) in the East Carpathians, Romania (Fig. 1). CGH represents the southeastern part of the Neogene-Pleistocene calc-alkaline magmatic province which accompanies the East Carpathians (Fig. 1, inset). Volcanic evolution in CGH differs significantly from other parts of the Carpathian Neogene calc-alkaline region by being the youngest and showing an obvious along-arc migration of volcanism since ~10 Ma (Pécskay et al. 1995a, 2006) from northwest toward southeast. As a whole, CGH volcanism is characterized as being post-collisional (e.g., Seghedi et al. 2004, 2011), derived after

convergence and the soft collision of the Tisza-Dacia microplate with the western margin of the large Eurasian plate at ca. 10 Ma (Maţenco and Bertotti 2000; Maţenco et al. 2007).

The special characteristics of South Harghita Mts., as compared with the rest of CGH, consist of crosscutting relationships with the Carpathian fold-and-thrust structures of its basement, thicker crust, the youngest ages, and progressively increasing alkalinity of the magmas (e.g., Szakács et al. 1993).

Ciomadul volcano: general features

The Ciomadul volcanic edifice is a dome complex built on top of folded and thrustured Lower Cretaceous flysch units, where a central cluster of domes hosts two explosion craters. A number of isolated peripheral domes and an intrusive body encountered at 575 m depth by a drilling complete the picture (Figs. 2 and 3). Lava domes, coulées, and lava flows are the main volumetric components of the volcanic edifice. The lithological features of the proximal volcanoclastic rocks have partly been described by Szakács and Seghedi (1989), Szakács and Jánosi (1989), Juvigné et al. (1994), Moriya et al. (1995, 1996), and Vinkler et al. (2007), while basic information on distal deposits belonging to the volcano was provided by Bányai (1917), Casta (1980), and Teulade (1989).

The prevailing rock type of the volcano is high-K dacite (Szakács and Seghedi 1986; Mason et al. 1996). Plagioclase (An_{85-30}), biotite (13.5–18 % annite), and amphibole (mostly calcic hornblende) are the main phenocryst phases. Pyroxene,

corroded quartz, apatite, and sphene are the main accessory minerals found in some dome lavas. Rarely, high-Mg pyroxene and olivine inclusions are found within the amphibole (Vinkler et al. 2007). Common phases of the groundmass are plagioclase and K-feldspar (sanidine, $Or=60-65$). The main geochemical characteristics of Ciomadul rocks have been discussed and interpreted in previous contributions (Peltz et al. 1987; Seghedi et al. 1986, 1987, 2011; Mason et al. 1996, 1998; Harangi and Lenkey 2007; Vinkler et al. 2007).

Structure of the volcanic edifice

Ciomadul volcano is developed over an area of 80 km² (Table 4). As a whole, it can best be characterized as a volcanic dome complex (Szakács and Seghedi 1995; Lexa et al. 2010).

The volcanic structure is dominated by a central group of tightly packed domes partly surrounded by a number of isolated peripheral domes to the north (Haramul Mic) and the east (Bálványos, Búdös/Puturosul, Dealul Mare). The Bába Laposa dome is located to the northwest from the central group of domes, on the western side of the Olt valley (Fig. 2); its structural position (part of Pilişca volcano or Ciomadul) was up to now unclear. However, the petrography and relatively old K–Ar age of its rocks (i.e., 1.46 Ma, Fig. 2) indicate that it is probably part of Pilişca.

The central dome cluster shows a roughly elliptical outline whose long axis trends in the NNE direction, consistent with

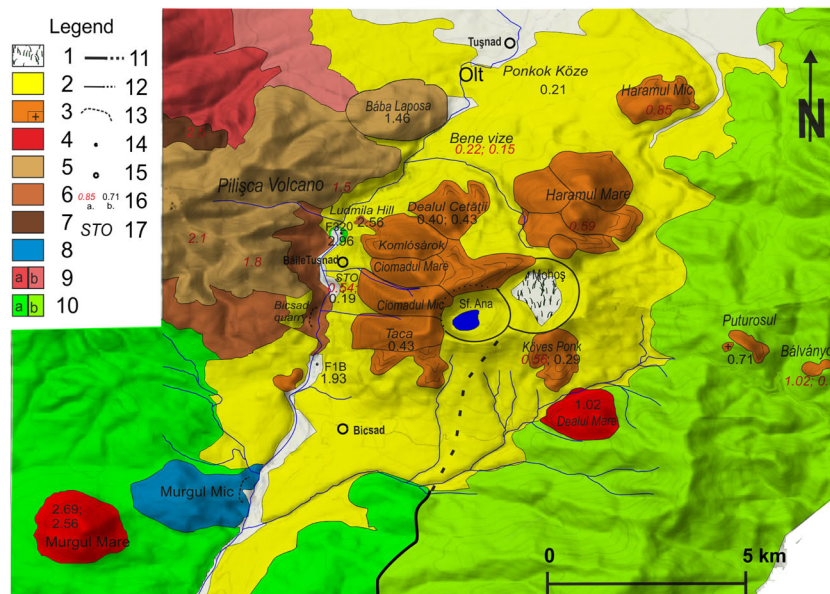
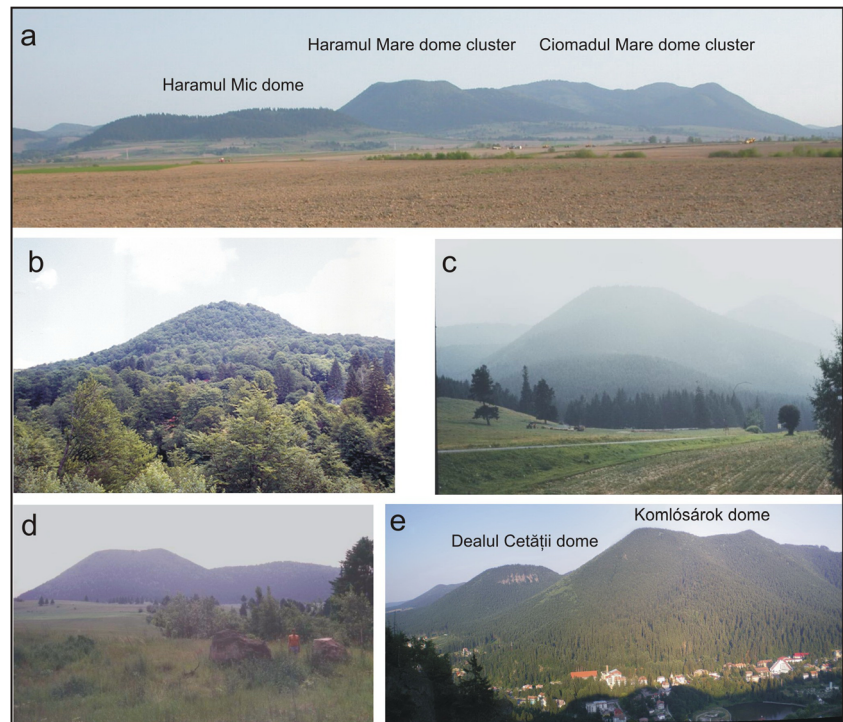


Fig. 2 Geological map of Ciomadul volcano. Legend: 1, Mohoš swamp; 2, Ciomadul volcano—volcanoclastic deposits; 3, Ciomadul dacite domes; “+” intrusion; 4, andesite dome (Dealul Mare); 5, Pilişca volcano—andesite and dacite domes; 6, Pilişca volcano—andesite with amphibole and pyroxene; 7, Pilişca volcano—basaltic andesite (Mitaci

type); 8, Shoshonite (Murgul Mic dome); 9, Cucu volcano: *a* andesite with amphibole±biotite; *b* volcanoclastic deposits; 10, Cretaceous flysch deposits: *a* Tithonic-Neocomian; *b* Barremian-Albian; 11, fault; 12, crater outline; 13, quarry; 14, drilling; 15, town; 16, K–Ar age; 17, STO-South Tuşnad Outcrop

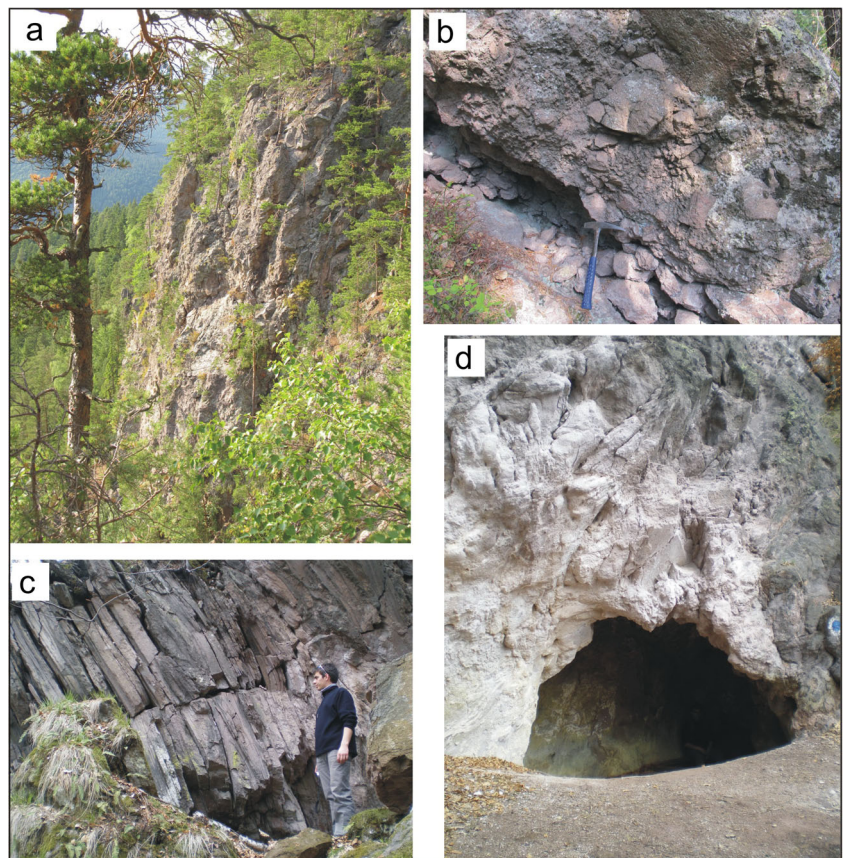
Fig. 3 Morphological features of the Ciomadul dome complex. **a** Ciomadul volcano as seen from the North; **b** Bálványos dome; **c** The Haramul Mare dome cluster, seen from the east; **d** Haramul Mare dome; **e** Ciomadul domes as seen from across the Olt river (west); Băile Tușnad Spa in the foreground



the strike of the major structural features of the area (Fig. 2). Most of the present-day dome summits (presumably

representing their former vents) are aligned in the same direction.

Fig. 4 Dome rocks. **a** Coarse dome-envelope breccia exposed in a steep cliff on the southern flank of the Dealul Cetății dome; trees 8–10 m high on top of the cliff for scale; **b** detail of Dealul Cetății dome breccia. Slight inclined bedding is visible. A larger breccia block (*above hammer for scale*) displays polygonal shape and short peripheral radial cracks on one of its margins; **c** dome lava rock outcrop in the northeastern flank of Puturosul dome remnant showing inclined slightly curved and densely packed platy jointing; person for scale; **d** Puturosul dome lava rock with fumarolic alteration (*discolored*) above cave; deposition of sulfur is visible in the cave interior; blue tourist path sign (12 cm across) on the right for scale



The domes

Volcanic domes of Ciomadul volcano show a variety of features in terms of position, age, aspect ratio, degree of erosion, and evolution.

The two easternmost isolated domes—Bálványos (Fig. 3b) and Búdös/Puturosul—cover a small surface (Fig. 2), and their rugged topography is dominated rather by erosion than by original dome morphology. At Búdös/Puturosul, a thermal contact zone with the pierced flysch sediments including hornfels is exposed some 200 m south from the main body of the dome (Fig. 2). The Búdös/Puturosul dome dacite is locally flow-banded and platy-jointed (Fig. 4c) and shows pervasive fumarolic alteration features (Fig. 4d). Bálványos and Búdös/Puturosul are interpreted as erosional remnants of former domes.

Two sub-clusters of domes can be recognized within the central group, each composed of a number of amalgamated individual domes: the Ciomadul Mare group and the Haramul Mare group (Fig. 2). Most of the Ciomadul domes, excepting Bálványos and Búdös/Puturosul, and some partially destroyed central-group domes (e.g., Köves Ponk), preserve relatively well their original morphology, with insignificant post-eruptive erosional overprint. With the notable exception of Haramul Mic and Bába Laposa, they are high aspect-ratio (height-diameter ratio) domes with steep outer slopes (Fig. 3c–e). Downward decreasing slopes outlining almost perfect upward-concave profiles, resembling those of composite volcanoes, can be seen at the Dealul Cetății dome (Fig. 3), resulting from redistribution of the remnants of dome crumble and talus debris toward the low-lying bases of the dome.

The lower slopes of the domes facing the Olt valley are more modified by erosion (i.e., steepened) than those farther on from the valley. Most of the dome summits display rounded topography (Fig. 3d) probably as a result of erosional overprint on the original topography. They have been characterized as being of Peléan type (Karátson et al. 2013). However, there are domes with flat or even slightly concave summits (e.g., Dealul Cetății dome, Fig. 3d) suggesting the existence of former craters related to episodic explosive activity accompanying dome growth.

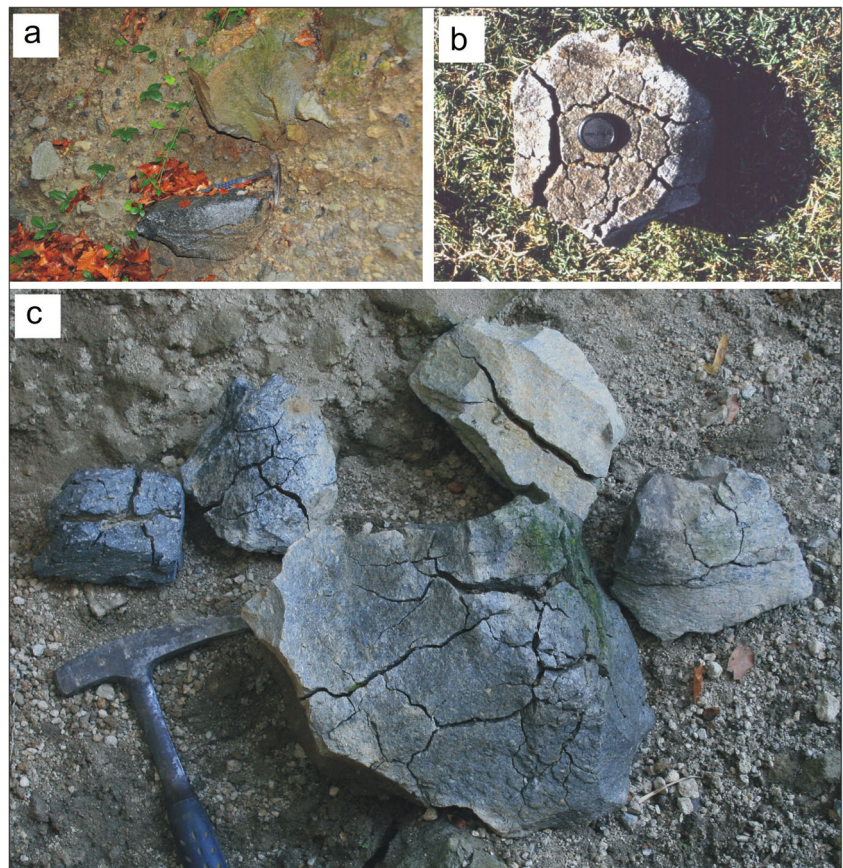
At present, the domes generally lack a dome-envelope breccia, either because they never existed or because they have been removed by erosion after dome growth was completed. Dealul Cetății is the notable exception, where an Olt river-facing scarp exposes dome-envelope breccia (Fig. 4a, b) at ca. the upper 1/3 of the dome slope. Other remnants of envelope breccia may well exist at other locations hidden under the thick vegetation cover.

Haramul Mic (Fig. 3a) and Bába Laposa are isolated flattened lower aspect-ratio domes. They display large summits and lower slopes.

The central dome cluster displays a much more complicated topography, resulting from amalgamation of several closely packed domes growing roughly during the same time. Occasional generation of other effusive features, such as coulées and short lava flows, further complicate the volcanic structure. One coulée, well seen from the west, formed from lava that oozed out from between two high aspect-ratio domes (Fig. 3d). At the southwestern part of the cluster, a short thick lava flow extends southwards from the Taca dome (Fig. 2). The domes located in the inner part of the group were destroyed during late-stage explosive eruptions, leaving behind only their topographic remnants (e.g., Ciomadul Mare and Köves Ponk).

Decimeter-sized cracked polygonal blocks resembling bread-crust bombs are found as loose blocks mostly in valley bottoms draining the southern flank of the volcano (Fig. 5). They can be grouped in three categories: (a) entirely or mostly glassy bombs, dark colored with radially arranged cracks and no contrasting porous interior and glassy margin (Fig. 5a, b), (b) typical bread-crust bombs with lighter-colored porous interior and dark-colored glassy rinds of various crack density, width, depth, and pattern; some of them greater than 1 m across, and (c) massive, non-glassy, light colored, and rindless blocks with a network of shallow and narrow cracks. Most of them show polygonal shape (Fig. 5b, c), and many of them are platy (Fig. 5b). Both concave and convex faces can be seen. Flow banding is clearly visible in part of the bombs. Rare outcrops of volcanoclastic deposits containing these “volcanic bombs and blocks” (Szakács and Jánosi 1989) can be examined. The largest of them (found on the southern slopes of the volcano) show a matrix-supported massive deposit with centimeter-sized dacite clasts of various alteration colors and a few larger, decimeter-sized cracked dacite blocks (Fig. 5a). No geometric relationships with any other deposits underlying or overlying it can be seen there. It can be interpreted as a debris flow deposit rather than a primary pyroclastic deposit. Bread-crust bombs are traditionally interpreted as resulting from Vulcanian-type explosive eruptions (e.g., Wright et al. 2007). Their occurrence at Ciomadul volcano only in debris flow deposits, as found so far, and the variety of their geometric features raises questions about how they are related to dome-forming processes. However, isolated Vulcanian episodes punctuating the dome growth processes, followed by reworking of the resulting fragmental material in debris flows in which dome-rock clasts with surficial cracks (such as that in Fig. 4b) were admixed, can also be envisaged. Wohletz and Heiken (1992) note that Vulcanian explosions may occur periodically during both growth and destructive phases of dome activity. We conclude that the three different types of bombs present at Ciomadul cannot be ascribed to a unique formation mechanism. The eruptive centers from which the inferred Vulcanian explosive episode(s) likely occurred are

Fig. 5 Bread-crust bombs of Ciomadul volcano. **a** Two small bread-crust bombs in a massive unsorted volcanoclastic (debris flow?) deposit cropping out in a brook on the southern slopes of the volcano; both of them show radial cracks; the dark-colored bomb below is glassy; hammer for scale; **b** densely cracked six-sided flat polygonal bread-crust bomb; lens cap for scale. **c** Collection of bread-crust bombs from the southern slopes of Ciomadul (photo courtesy by Alpár Kovács); hammer for scale



the Köves Pank or Taca, the nearest domes situated to the north (Fig. 2).

The craters

The two craters disrupting the central dome cluster of Ciomadul are different in size and shape. Their age relationships are obvious from their mutual spatial positions. As seen on the simplest topographic map, the circular depression of the Sf. Ana crater disrupts the larger depression hosting the Mohoş swamp (Figs. 2 and 6a, b). The younger Sf. Ana crater (Fig. 6b) is ca. 1.5 km in diameter and ca. 118 m deep (lake level relative to the lowest crater rim at the Mohoş-Sf. Ana saddle) and hosts Sf. Ana crater lake. Currently, the lake is only 7 m deep (Magyari et al. 2009), while 11 m were measured ca. a century ago (Cholnoky 1922). In contrast, Mohoş is larger (ca. 1.9 km in diameter, Fig. 6a), bowl-like and much shallower (ca. 20 m, peat-bog surface relative to the Mohoş-Sf. Ana saddle). It is partly filled with the Mohoş swamp and peat-bog, ca. 10.5 m thick (Tanţău et al. 2003). Their different morphological features suggest different origin (i.e., different styles of explosive eruptions).

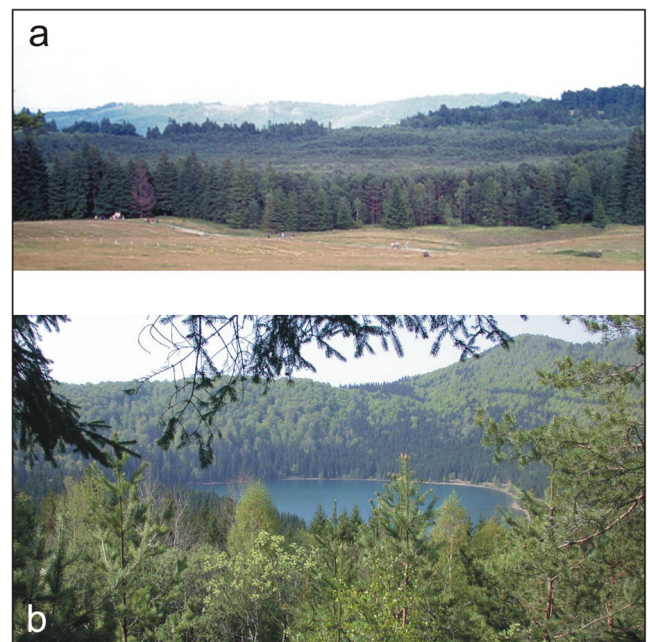


Fig. 6 Craters of the Ciomadul volcano. **a** The phreatomagmatic Mohoş crater hosting a peat-bog as seen from the saddle between the two craters; **b** Sf. Ana lake at the bottom of the Sf. Ana crater formed during the Plinian eruption as seen from its northern upper slopes. The Taca dome is visible bordering its southwestern margin (*upper right*)

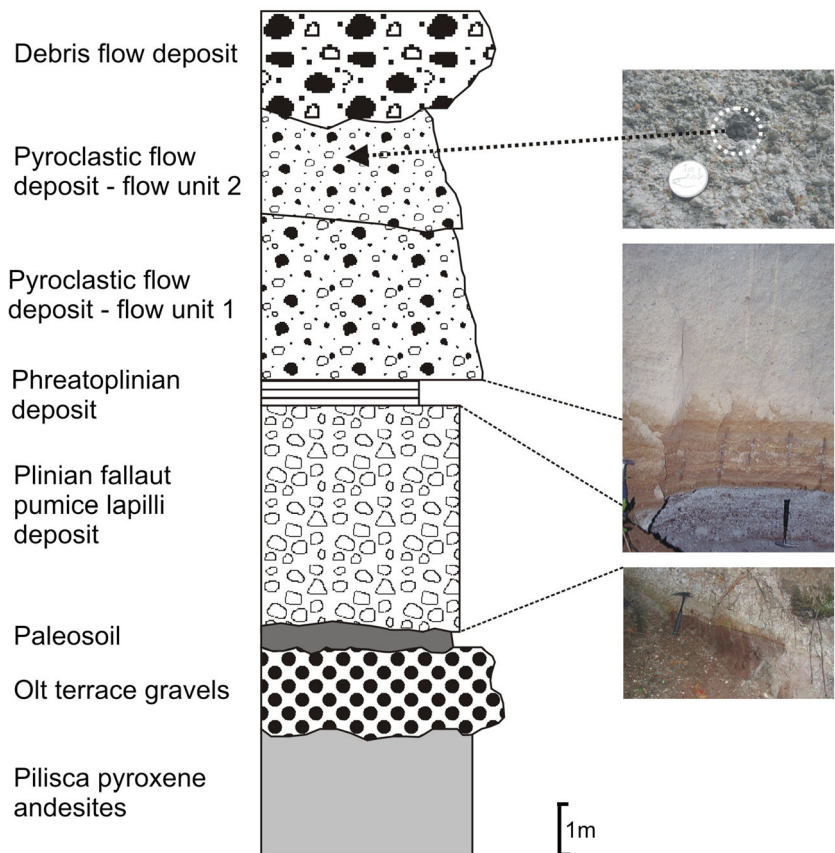
Proximal volcanoclastic deposits

Exposures of volcanoclastic deposits are found close to the Mohoş crater rim and at the southern and eastern peripheries of the dome complex. A key sequence of volcanoclastic deposits crop out south of Băile Tuşnad Spa, where a composite lithological column can be constructed (Fig. 7). The sequence's upper part has been described previously by Teulade (1989), Moriya et al. (1996), and Vinkler et al. (2007). The sequence consists, from base to top, of the following lithological units:

- (a) Massive, dark gray-colored pyroxene andesite lavas are exposed in the eastern Olt river bank for at least 2 m thickness. Similar rocks were found in a borehole (FB1, Fig. 2), a few kilometers to the south. Interpretation: since the rocks are identical in composition with the pyroxene andesites exposed in the Bicsad quarry (Fig. 2) and since they are unknown farther east in the area of Ciomadul volcano, we interpret them as belonging to the older Pilişca volcano (Szakács and Seghedi 1995);
- (b) Coarse gravel deposits (Fig. 7) containing, among pyroxene andesites, rounded Ciomadul dacite lava clasts. The same gravel layer, at least 2 m thick, exposed a

- couple of meters higher at the base of the south of Băile Tuşnad outcrop.. Interpretation: taking into account its position and outcrop area, it is clear that the gravels represent Olt valley terrace deposits emplaced in a time period during which Ciomadul was already active;
- (c) Gray-colored, organic matter-poor paleosoil horizon ca. 40 cm thick (Fig. 7). It was sampled and its radiocarbon age determined as reported in Moriya et al. (1996). Interpretation: the paleosoil probably developed along the Olt river terrace in the time interval between the dome-building phase and the late explosive phases of Ciomadul or, alternatively, during part of the dome phase in an area topographically shadowed from deposition of dome-related material;
- (d) A 4.6-m-thick coarse pumice block and lapilli layer (Fig. 7) containing sparse dacite lithic blocks. The deposit is clast-supported and generally well-sorted with pumice clasts of 6 to 20 cm in size. Vague diffuse layering can be seen with slight clast-size variations across the layer. The sorted nature of the deposit is locally disturbed by the presence of larger-sized dacite lithic clasts. Interpretation: according to Szakács and Seghedi (1996) and Vinkler et al. (2007), it is a proximal (sub)plinian pumice fall deposit quickly removed on the steep dome slopes and deposited at lower dome-feet

Fig. 7 Lithostratigraphic relationships and lithological features of volcanoclastic rocks of Ciomadul volcano as seen in the outcrop South of Băile Tuşnad (location STO on Fig. 2). Photos on the right side illustrate lithostratigraphic units represented in the lithological column (left). The circle in the upper picture highlights a charcoal piece embedded in the upper pyroclastic flow depositional unit (see text)



locations. Its grain-size characteristics confirm the fall-out origin and reflect the proximal origin of the deposit, while the chemical composition of the pumice clasts show stronger similarities with Sf. Ana volcanics than with those originating from Mohoş (Teulade 1989);

- (e) A 45-cm-thick sequence of thinly (cm)-bedded finer and poorly sorted tuff and lapilli tuff deposits (Fig. 7) with both gradational base and top which still preserves the clast-supported feature of the underlying pumice lapilli layer to which it strikingly contrasts. The clast composition is identical (dacite pumice) to that of the underlying deposit, excepting for a higher degree of alteration and higher density (less porosity). Interpretation: in agreement with previous interpretations (Szakács and Seghedi 1996 and Vinkler et al. 2007), we consider them as pyroclastic fall deposits resulting from a short phreatomagmatic episode of the eruption marking the transition between the Plinian fall phase and the following explosive phase. This was probably the event which destabilized the Plinian column and drove it toward collapse and generation of pyroclastic density currents. The lack of observable discontinuity or unconformity separating the deposit from the lithological units below and above strongly suggest that these explosive phases succeeded rapidly after each other, belonging to a unique continuous explosive eruption;
- (f) Thick (ca. 5.5 m) massive and unsorted matrix-supported pumice and lithic block-rich lapilli-tuffs containing a large variety of clasts showing different colors, degrees of alteration, porosity, and density, but all of the same hornblende biotite dacite composition. A slightly undulating surface resembling an unconformity separates the deposit into two units of roughly identical thickness (Fig. 7). Slight normal gradation of pumice clasts, whose frequency increases upwards in both subunits, can be observed, while denser clasts seem not to be graded. Pieces of charcoal (Fig. 6) collected for radiocarbon dating were found only in the upper subunit. Interpretation: the features described above point to en-mass emplacement of the fragmental material from pyroclastic density currents resulting in two pyroclastic flow-type depositional units. That suggests that at least two waves of density currents following each other were generated by the Plinian eruption column collapse.
- (g) The uppermost unit of the sequence is separated by a prominent erosional unconformity (channel). It is a massive matrix-supported unsorted deposit, containing angular to subrounded blocks of mostly massive dacite, some with obvious alteration crust embedded in a mass of finer sand-like material of the same composition. Block and gravel-sized clasts look heterogeneous in color, shape, and degree of alteration. No non-volcanic material was recognized within it. Interpretation: this is a

debris flow deposit emplaced on top of the pyroclastic flow units shortly after the explosive eruption ceased.

The described sequence shows that the generating explosive eruption consisted of a succession of phases, starting with a (sub)Plinian pumice fall event, followed by a phreatomagmatic episode leading to the collapse of the eruption column and generation of pyroclastic flows in at least two distinct episodes, then mixture of the loose tephra with water-generated debris flow deposits capping the pyroclastic sequence.

Phreatomagmatic pyroclastic deposits occur near the northeastern rim of the Mohoş crater (Fig. 8). They were exposed in two small quarries located above each other. The deposits seen in the lower quarry (since destroyed) have been described as typical fine accretionary lapilli-bearing base-surge deposits with fine lamination and dune-like structures (Szakács and Seghedi 1989) (Fig. 8a, b). In contrast, the upper quarry displays coarser unsorted deposits, rich in pumice and lithic blocks and lapilli (some of them glassy) within a coarse tuff matrix whose grain-size variations result in a clear bedding feature (Fig. 8c). They have been described by Vinkler et al. (2007), who observed sparse impact structures and interpreted them as alternating pyroclastic fall and surge deposits of phreatomagmatic origin. Transport direction indicators of both outcrops show their origin from the nearby Mohoş crater (Szakács and Seghedi 1989; Vinkler et al. 2007). Overall, the Mohoş crater-rim deposits suggest a more energetic early phase generating the base-surge deposits (higher level of fragmentation) followed by a less energetic phase likely due to changing (diminishing) magma-water ratio. Phreatomagmatic deposits can also be seen at more distal locations, such as the roadside outcrop near Turia, where horizontally bedded sequences of fallout and base-surge deposits show an overall finer grain size and reduced thickness (Fig. 8d).

Distal pyroclastic deposits

There are no pyroclastic deposits (e.g., tuffs) which can be interpreted as originating from Ciomadul volcano at distal locations exceeding 50 km. Only two exposures of Ciomadul lapilli layers are known at a distance of ca. 40 km to the east, both in the town of Târgu Secuiesc (Bányai 1917). They are considered here “distal,” according to Szakács et al. (2002). In both outcrops, a ca. 20–23-cm-thick pumice lapilli layer is interbedded in Upper Pleistocene sand deposits. The grain-supported deposit consists of well-sorted pumice clasts of 2.0–2.5 cm in diameter (with 5 cm maximum size, Vinkler et al. 2007) and massive internal structure (Fig. 9). It was apparently deposited as a single fallout unit originating from a (sub)Plinian eruption. The eruption center from which these



Fig. 8 Proximal phreatomagmatic deposits in outcrops near the eastern margin of the Mohoș crater. **a** Dune-bedded base-surge deposits originating from a pyroclastic density current flowing from left to right (i.e., from the crater center away); hammer for scale is 70 cm long; **b** detail of **(a)** showing accretionary lapilli; lens cap for scale; **c** alternating beds of coarser grained fall deposits and finer grained surge deposits at the Mohoș crater rim overlying the base-surge deposits seen in **(a)**. Bedding

is inclined in a direction away from the Mohoș crater. Some slightly pronounced impact sags are also visible (*arrows*); hammer for scale. **d** Phreatomagmatic deposits in a more distal location (*on the Bălványos-Turia roadside, east of the Mohoș crater*) showing an overall finer grain size and more diffuse limits between beds of coarser fallout and finely laminated base-surge deposits; note that bedding is almost horizontal; hammer for scale

deposits originated is uncertain. Pumice composition is different from that of the south Băile Tușnad fallout pumice, showing higher silica content and lower An% of plagioclase than those assigned to the Sf. Ana eruption (Vinkler et al. 2007).

Epiclastic deposits

Epiclastic deposits are widespread at the volcano's northern and southern peripheries. A sand quarry at Ponkok Kőze exposes a thick epiclastic sequence (Fig. 10b) mostly consisting of sand-sized particles of Ciomadul dacite and its component minerals (plagioclase, biotite, and amphibole). They display a large variety of sedimentary structures characteristic of shallow water environments, such as fine lamination, cross-bedding, chute-and-pool structures, and unconformities. Riverbed and Olt terrace gravel deposits south of Bicsad village frequently contain Ciomadul material. High-level terrace deposits and debris flow deposits, exposed on the western side of

the Olt valley, mostly made of Ciomadul volcanics, overlie Pilișca lavas as seen in the Bicsad quarry (Fig. 10a). They represent land-deposited epiclastic volcanic material of Ciomadul volcano. As a whole, epiclastic deposits found at the volcano peripheries can be interpreted as originating from removal and redeposition in ring-plain environments of the effusive and, mainly, explosive products of Ciomadul volcano.

Geochronology

Historical summary

The “youthful” steep topography of Ciomadul and its crater lake suggested to early twentieth century researchers that the volcanic edifice was probably younger than any other volcano

Fig. 9 Distal pyroclastic deposits of Ciomadul volcano in the outcrop at Târgu Secuiesc. **a** General view of the outcrop with the prominent pumice lapilli layer, ca. 20 cm thick; persons for scale; **b** detail of **(a)** showing sharp base and diffuse reworked top of the pumice lapilli layer; shovel for scale



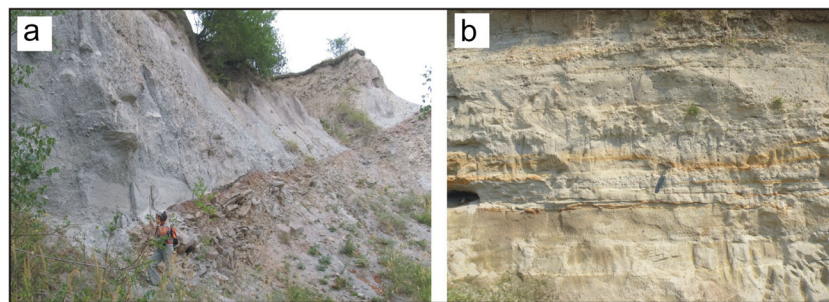


Fig. 10 **a** Bedded reworked Ciomadul pyroclastic rocks covering Pilișca pyroxene andesites in the Bicsad quarry (see map in Fig. 2). Debris flow depositional units can be seen in the middle part of the volcanoclastic sequence. Note the unconformity between bedding and contact surface of the andesite, suggesting a depression of the paleo-topography (*centered*

somewhere left from the picture) in which the volcanoclastics were accumulated and preserved; person for scale. **b** Sequence in reworked finely bedded volcanoclastic deposits exposed in a “sand” quarry north of Tușnad; hammer for scale

of the CGH range. Since volcanic products having compositions similar to that of the Ciomadul rocks have been encountered in terrace deposits of the Olt river, a Pleistocene age was assumed by most of them (e.g., Cholnoky 1922; Székely 1959). Bányai (1917, 1964), however, favored an Upper Pliocene age.

Although it was largely accepted that Ciomadul is the youngest volcano of the range, its actual age and especially its chronological evolution remained poorly understood until radiometric methods started to be used for dating. The results of the first K–Ar age determinations for Ciomadul rocks were published by Casta (1980), then by Pécskay et al. (1992). Radiocarbon dating started to be used almost in the same time (Juvigné et al. 1994) after the discovery of charcoal fragments in pyroclastic density current deposits. Since then, an ever growing number of radiometric age data have been obtained (Pécskay et al. 1995b; Moriya et al. 1995, 1996; Vinkler et al. 2007; Harangi et al. 2010). Attempts of Ar–Ar dating have also been made (e.g., Karátson 2007) to refine the geochronological picture of volcano evolution.

Existing data

K–Ar data

Previously published K–Ar data on Ciomadul volcanic rocks are displayed in Table 1. Most of them have been obtained at the K–Ar Laboratory of ATOMKI, Debrecen, Hungary (Pécskay et al. 1992, 1995b).

Ar–Ar data

The results of two Ar–Ar age determinations on biotite monomineralic fractions have been published (with no analytical details) by Karátson (2007). One of them ($T_4=0.474\pm 0.049$ Ma) was obtained from a pumice-like lithic clast taken from pyroclastic flow deposits of the South Tușnad outcrop. Its age is similar to that of the biotite found in the same

deposit, as determined by the K–Ar method ($AM_2=0.540\pm 0.019$ Ma) (Pécskay et al. 1995b). The other sample, collected from an outcrop at the northern margin of Mohoș swamp, yielded 0.270 ± 0.02 Ma. Both ages likely reflect the timing of dome-building episodes, since the clasts already existed when incorporated in the pyroclastic flow deposits.

U–Pb and (U–Th)/He geochronology

Karátson et al. (2013) recently published new radiometric age data for zircon crystals from Ciomadul rock samples based on the U–Pb and (U–Th)/He methodology. According to their preliminary results, “U–Pb ages show a broad scatter and large variation even in individual samples.” The single-crystal ages from the crater rims range mostly between ~160 and 60 ka, while for the pumiceous deposit, the variation is even larger, from ~180 to 40 ka. The scatter is significantly larger than the uncertainty of the “individual ages.” The authors interpret

Table 1 Published K–Ar data on Ciomadul volcanic rocks

Sample	Location	Rock type	Rock body	K–Ar age (Ma)	Reference
	Haramul Mic	Dacite	Lava dome	0.85	Casta (1980)
HR13	Bálványos	Dacite	Lava dome	0.92 ± 0.18	Pécskay et al. (1995b)
				1.02 ± 0.15	Pécskay et al. (1995b)
AM43A	Haramul Mare	Dacite	Lava dome	0.59 ± 0.16	Pécskay et al. (1995b)
AM35	Köves Ponk	Dacite	Lava dome	0.56 ± 0.11	Pécskay et al. (1992)
AM2	South Tușnad	Dacite	Pumice clast	0.54 ± 0.19	Pécskay et al. (1995b)
AM-SZ	Bene vize	Dacite	Block	0.15 ± 0.05	Pécskay et al. (1992)
				0.22 ± 0.06	Pécskay et al. (1992)

these results as representing “pre-eruptive crystallization ages” of the dated zircon crystals. The (U–Th)/He ages of zircons from the dome rocks are around 40 and ~100 ka, respectively, while the samples from the pumice-bearing pyroclastic deposits of the youngest explosive phase “yielded apparent (U–Th)/He ages around 40 ka.” The authors emphasize that their ZrHe ages “are uncorrected minimum ages.” Despite the uncertainties mentioned, they conclude that their “comparative morphometry and radiometric chronology” constrain the volcanic activity in Ciomadul to “between ~200/250 and 30 ka,” with emplacement of most lava domes ~150–100 ka (Karátson et al. 2013).

Radiocarbon data

Organic materials found in the youngest eruptive products and in deposits underlying or overlying them were analyzed by radiocarbon method in various laboratories. Charcoal pieces collected from pyroclastic flow deposits yielded radiocarbon ages published by Juvigné et al. (1994), Moriya et al. (1995, 1996), Vinkler et al. (2007), and Harangi et al. (2010). ^{14}C ages of organic material in paleosoil underlying the South-Tuşnad pumice fall deposit were obtained by Moriya et al. (1995, 1996).

Sf. Ana lake bottom sediments were dated by Magyari et al. (2006) using their organic content, while radiocarbon ages of Mohoš peat-bog material were published by Juvigné et al. (1994) and Tanţău et al. (2003). Magyari et al. (2006) have undertaken a multi-proxy investigation carried out on the sediment of the Sf. Ana crater lake bottom sediments.

The published radiocarbon age data are presented in Table 2.

Biostratigraphy data

In addition to radiocarbon dating, Sf. Ana lake bottom sediments were subjected to detailed biostratigraphical

investigation by Buczkó and Wojtal (2007) and Buczkó and Magyari (2007) mainly based on diatom flora and pollen analysis which roughly confirms the tephro-chronological data (Juvigné et al. 1994), suggesting that lake sedimentation was active at the end of the Late Glacial (0.12 Ma).

New K–Ar radiometric age determinations

Fourteen new K–Ar age data are presented here in order to complete the picture of volcanic evolution during the dome-building stage. Samples were collected from natural outcrops and drillcores.

Methodology The new K–Ar ages have been obtained at the K–Ar laboratory of the Institute for Nuclear Research, Debrecen, Hungary. Whole-rock samples were optically examined, and their fresh parts retained, crushed and sieved. The 150–300- μm size fraction was washed and dried. Magnetic separator, heavy liquids, and hand-picking were used for mineral separation. One portion of the ready-made sample was ground in an agate mortar for potassium analyses carried out with flame photometry.

Details of our analytical methods have been reported by Balogh (1985), Pécskay et al. (2006), and Odin et al. (1982). K–Ar ages were calculated using decay constants suggested by Steiger and Jäger (1977). The inter-laboratory standards Asia 1/65, LP-6, HD-B1, and GL-O, as well as atmospheric Ar were used to control the measurements. All analytical errors are reported at the 1σ level.

It should be noted that analyses of rocks younger than 1 Ma sometimes involved a possible overestimate of the K–Ar ages when “whole rock” samples were dated. Measurements on separated phenocryst mineral fractions show that especially early crystallized minerals (e.g., pyroxene, hornblende, etc.) are responsible for the discordant ages (Cassignol and Gillot 1982; Lippolt et al. 1986). Consequently, care was taken in the

Table 2 Published radiocarbon age data for Ciomadul volcano

Locality	Material	^{14}C age (Ka)	Calibrated ^{14}C age BP (Ka)	Reference
South Tuşnad	Charcoal piece	10.7±0.18	13–12.59	Juvigné et al. (1994)
South Tuşnad	Paleosoil	42.65		Moriya et al. (1995)
South Tuşnad	Charcoal piece	35.67		Moriya et al. (1996)
South Tuşnad	Charcoal piece	35.52		Moriya et al. (1996)
East Bicsad	Charcoal piece	27.04±0.45		Vinkler et al. (2007)
East Bicsad	Charcoal piece	27.2±0.26	29.5±0.26	Harangi et al. (2010)
South Tuşnad	Charcoal piece	39.0	41.3	Harangi et al. (2010)
Mohoš peat-bog	Bottom peat	7.61±0.07		Juvigné et al. (1994)
Sf. Ana lake	Alnus seed	8.05±0.05	8.977–9.029	Magyari et al. (2009)
Sf. Ana lake	Bulk sediment	8.46±0.11	9.710–9.950	Magyari et al. (2009)
Sf. Ana lake			9.300	Magyari et al. (2009)

interpretation of the ages determined on monomineralic fractions since it gives the “age of crystallization” which can be significantly older than the age of the lava emplacement. We selected the most suitable samples with mineral phases crystallized at shallow depths or at the surface. In order to avoid this problem, coarse-grained phenocrysts, and especially xenocrysts/xenoliths, were removed during sample preparation.

Generally, the anomalously high $^{40}\text{Ar}/^{36}\text{Ar}$ ratios in Ar extracted from young volcanic rocks are explained by the presence of excess Ar. However, excess Ar is most commonly found in metamorphic rocks and where the fluids are derived from basement rocks in fluid-rich regimes (Vance et al. 1998), and it is much less common in volcanic systems, where outgassing to the atmosphere provides an effective release mechanism. On the other hand, small amounts of excess Ar may be present in quartz phenocrysts and in fluid and melt inclusions within them (Vance et al. 1998), but the volume of this Ar is negligible as compared with the radiogenic Ar accumulated in the rocks. A few of our analyzed samples contain juvenile quartz microphenocrysts.

The amount of radiogenic ^{40}Ar was determined by the isotope dilution method using ^{38}Ar as a spike. Consequently, for the age calculation, we have measured the $^{36}\text{Ar}/^{38}\text{Ar}$ and $^{40}\text{Ar}/^{38}\text{Ar}$ isotope ratios. The precise volume of the ^{38}Ar spike is determined by using international standards (LP-6., HD-B1., Asia 1/65).

Extra care was taken when atmospheric Ar contamination was obvious from the measured Ar isotope ratios. In this case the $^{38}\text{Ar}/^{36}\text{Ar}$ ratio should also be measured. This effect can be a serious analytical problem for the correct age interpretation (Krummenacher 1970). The contamination with atmospheric

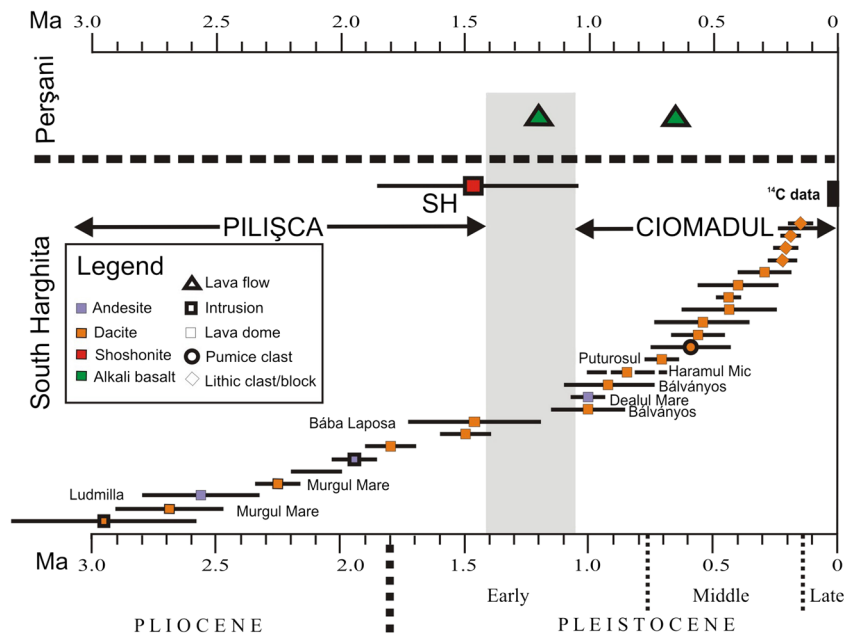
Ar seems to be correlated with the water content of the lavas, and it depends also on the conditions of cooling of the lava at the surface (Gillot 1984). We can exclude the significant presence of excess Ar in the studied volcanic rocks of Ciomadul, but a slight Ar loss cannot be ruled out completely due to the thermal effect caused by the episodic volcanic activity and subsequent insignificant hydrothermal activity. Therefore, their ages cannot be significantly younger than the result of our study. However, further analytical work has to be done on the youngest dome rocks (those of ca 0.2 Ma or less in age) to measure precisely the $^{38}\text{Ar}/^{36}\text{Ar}$ ratio which would determine the cause of the $^{40}\text{Ar}/^{36}\text{Ar}$ anomaly whenever detected.

Results The new K–Ar ages obtained on Ciomadul rocks are shown in Table 3, while K–Ar ages previously reported are given in Table 1. Figure 11 displays a summary of all available age data on Ciomadul in comparison with the age of neighboring volcanoes and of roughly coeval volcanism in the South Harghita and Perşani Mts. The K–Ar results reveal that most units mapped as belonging to Ciomadul volcano were erupted during a ~1-Myr age interval between ca. 1.0 and 0.15 Ma. The dome-building stage of the volcanic edifice started at ca. 1 Ma ago, the ages of the easternmost isolated dome Bálványos and Dealul Mare peripheral dome. The Bálványos dome age is constrained at ca. 1 Ma by the previously published analysis (Pécskay et al. 1995b). Slightly younger ages were obtained on other peripheral domes, Haramul Mic (0.85 Ma, Casta 1980) and on the eroded Büdös/Puturosul dome (0.71 ± 0.04 Ma). The central group of domes erupted over intervals of time ranging between 0.59 and 0.14 Ma (Szakács et al. 1993; Pécskay et al. 1995b).

Table 3 Results of K–Ar dating on Ciomadul volcanic rocks (this work)

Lab no.	Sample no.	Location	Rock type	Rock body	Dated fraction	K (%)	$^{40}\text{Ar}_{\text{rad}}$ (%)	$^{40}\text{Ar}_{\text{rad}}$ (ccSTP/g $\times 10^{-7}$)	K–Ar age (Ma)	Observation
5161	F320	F320-Tuşnad	Dacite	Intrusion	wr	2.02	10.9	2.336	2.96 ± 0.38	
3514	HR49	Murgul Mare	Dacite	Lava dome	wr	2.16	17.3	2.263	2.69 ± 0.22	
3512	HR46	Ludmilla Hill	Andesite	Lava flow (?)	wr	1.77	14.9	1.765	2.56 ± 0.24	
3515	HR50	Murgul Mare	Dacite	Lava dome	wr	2.28	51	1.999	2.25 ± 0.09	
7334	HRF1B/109	Drillcore (109m)	Andesite	Intrusion (?)	wr	1.51	.29.7	1.135	1.93 ± 0.09	
3513	HR47	Bába Laposá	Dacite	Lava dome	wr	2.97	7.4	1.691	1.46 ± 0.27	
3508	AM60A	DI. Mare	Andesite	Lava dome	wr	2.28	23.1	9.067	1.02 ± 0.07	
7333	HR-BD-2	Puturosul	Dacite	Neck	wr	2.81	.25.1	0.772	0.71 ± 0.04	
3506	AM20	Dealul Cetăţii	Dacite	Lava dome	wr	2.94	3.0	0.489	0.43 ± 0.19	
3507	AM50	Ţaţa hill	Dacite	Lava dome	wr	2.97	13.4	0.493	0.43 ± 0.05	
3506	AM20	Dealul Cetăţii	Dacite	Lava dome	wr	2.94	3.6	0.458	0.40 ± 0.16	
2881	AM18	S Köves Ponk	Dacite	Lava dome	Biotite	5.96	3.7	0.680	0.29 ± 0.11	
3510	AM83	Ponkok Köze	Dacite	Block	wr	2.91	5.6	0.239	0.21 ± 0.05	
3505	AM2LAF	South-Tuşnad	Dacite	Lithic clast	wr	3.17	7.9	0.278	0.19 ± 0.04	Reworked clast

Fig. 11 Overview of existing radiometric age data on Ciomadul rocks in comparison with the ages of the neighboring/coeval volcanoes active in Pliocene-Pleistocene times in the South Harghita and Perşani Mts. *SH* shoshonites. A time gap is suggested between Pilişca and Ciomadul volcanoes (*light gray shading*). The age data within the *black box* marked “¹⁴ages” are shown individually in Fig. 13. K–Ar data sources: Casta 1980; Peltz et al. 1987; Pécskay et al. 1992, 1995b, and this work (Table 3) for South Harghita and Ciomadul volcano, Panaiotu et al. 2004 for Perşani Mts. ¹⁴C data sources are listed in Table 2



Volume calculations and eruption rate estimates

In order to assess the magnitude and volumetric eruption rates at Ciomadul, we performed volume calculation of its effusive and explosive products. A 3D terrain grid (DEM) was generated by digitizing topographic maps of the study area at the scale 1: 50,000. The Dealul Piscului 1979/Stereo 70 coordinate reference system was used. The Ciomadul volcano target zone (surfaces where Ciomadul rocks are mapped) was cut from the 3D grid model and used for surface and volume calculations. SURFER (version 8) software was used in both DEM generation and volume calculations.

According to the results obtained (Table 4), the eruptive products of Ciomadul volcano presently occur as a surface area of 81.64 km², and their volumes sum up at ca. 8.74 km³, less than 15.3 km³ as suggested for the similar surface (80.9 km²) by Karátson and Timár (2005).

Table 4 Results of volume calculations

Rock body	Area covered on map (km ²)	Volume from surface data (km ³)
Puturosu dome remnant	0.28	0.17
Bálványos dome remnant	0.13	0.07
Haramul Mic dome	1.30	0.34
Haramul Mare dome cluster	5.32	2.28
Dealul Mare dome	1.49	0.57
Köves Ponk dome remnant	1.05	0.47
Ciomadul Mare dome cluster	9.67	4.22
Volcaniclastic rocks	62.40	0.62
Total	81.64	8.74

Most of the volume figure (8.12 km³, i.e., >92 %) represents dome rocks. No dense rock equivalents were calculated, although most samples show some porosity. The volume of all volcaniclastic rocks found within the Ciomadul massif is less than 1 km³ (i.e. 0.62 km³, Table 4). The calculated volume should be viewed as a conservative estimate because medial/distal fallout tephra volumes and post-emplacment erosional removal of volcanic material have not been considered. Therefore, we consider a total volume of ca. 9 km³ of magma erupted at Ciomadul is a reasonable preliminary estimation.

Discussion

Ciomadul is already known as one of the youngest volcanoes in the whole CPR (e.g., Pécskay et al. 2006); however, the actual age range of its activity was largely unknown. The new radiometric ages, together with published data of Ciomadul, allows us to consider the age of this volcano and its eruptive history on more robust grounds.

The age of Ciomadul volcano

The main problem when discussing the age of Ciomadul volcano is to distinguish between the eruptive products of the volcano from those belonging to neighboring volcanoes, particularly Pilişca. The present-day natural geographical boundary between the two volcanoes is the Olt valley (Fig. 2). The lower part of the Pilişca edifice mostly consists of effusive products of amphibole-pyroxene andesite to

basaltic andesite composition. Furthermore, in the key section south of Băile Tuşnad, the spatial relationships are clear: Olt terrace sediments cover the Pilişca lavas and are in turn covered by a paleosol underlying Ciomadul pyroclastic deposits (Fig. 7). The upper part of Pilişca is, however, composed of andesitic-dacitic lava domes emplaced on top of the more mafic edifice base. Located in between Pilişca and Ciomadul (Fig. 2), Bába Laposa andesitic-dacitic dome's K–Ar age is ca. 1.5 Ma, significantly older than the oldest Ciomadul dome rocks and identical with the youngest of the Pilişca dome rocks. Similarly, the amphibole-pyroxene andesites in the Ludmilla Hill (Fig. 2), which differ both in K–Ar age (ca. 2.5 Ma) and in composition (medium-K andesites) from the Ciomadul rocks, can be reasonably assigned to the Pilişca volcano. The third ambiguous case is represented by the intrusive rocks encountered in a drillcore at Băile Tuşnad, whose composition (high-K dacite), as well as geographic position is compatible with both Pilişca and Ciomadul. However, its much older K–Ar age (2.96 Ma) precludes it from being assigned to the Ciomadul system.

Taking into account the arguments presented above and according to the radiometric (both K–Ar and radiocarbon) dating, the volcanic products of Ciomadul display an age range between ca. 1 Ma and a few tens of kiloannus, bracketing a volcanic evolution of roughly 1 Myr (Figs. 11 and 12). Comparing with the age ranges of the neighboring volcanic structures (Pilişca, Murgul Mare, Murgul Mic), it is

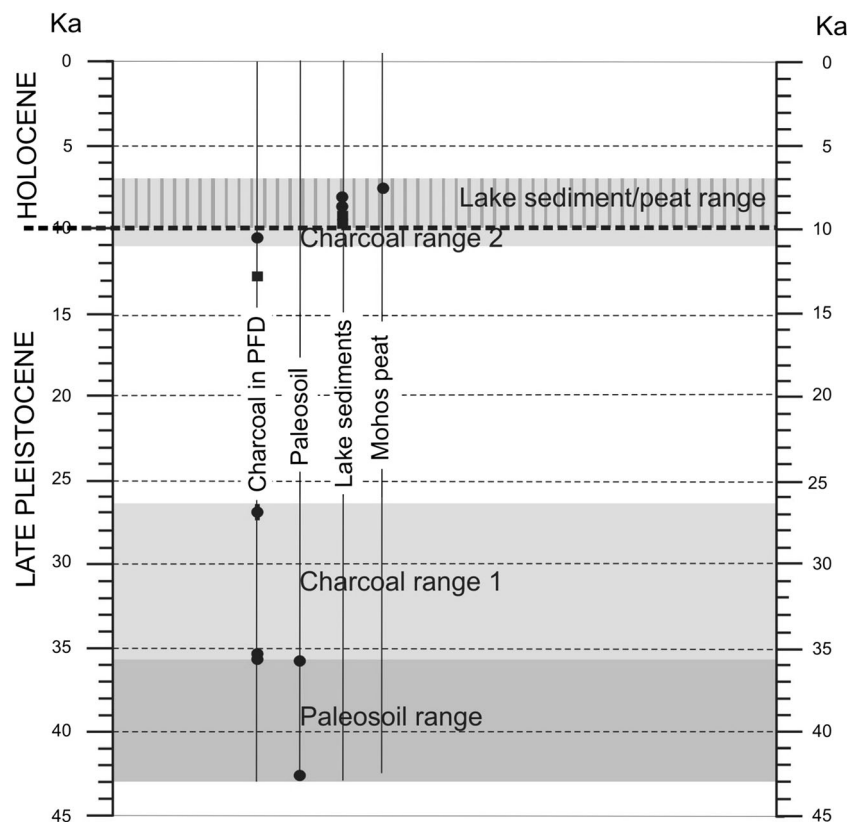
obvious that the eruptive history of Ciomadul postdates that of all other volcanoes in South Harghita Mts. and in the whole CGH range. Furthermore, Ciomadul started to be active with a gap of ca. 0.5 Myr after the most recent neighboring volcanoes became extinct (Fig. 11). In the context of geographic distribution, Ciomadul continued the southeastern extension of the CGH range. The intrusive rocks found at Băile Tuşnad by drilling document this spatial shift from Pilişca to Ciomadul sites, although the magmas did not arrive at the surface.

The claim of Karátson et al. (2013) that the volcanic activity of Ciomadul occurred between ~200/250 and 30 kyr, with most of the lava domes emplaced at ~150–100 kyr, is poorly substantiated by their preliminary U–Pb and (U–Th)/He age data, since (1) their radiometric ages obtained stand as “uncorrected minimum ages”, and (2) their samples belong only to rocks of the central dome complex of Ciomadul, while peripheral domes were not considered either for dating (Dealul Mare, Búdös/Puturosul, Bálványos), or for interpretation (Haramul Mic).

Volcanic evolution

The dome-building stage of the volcanic structure started at ca. 1 Ma, the age of both peripheral Bálványos (Pécskay et al. 1995a) and Dealul Mare domes, then shifted to the northerly Haramul Mic dome (0.85 Ma, Casta 1980) and to Búdös/Puturosul (0.71 Ma) followed by the main phase giving rise

Fig. 12 Summary of radiocarbon ages concerning the most recent activity of Ciomadul volcano (data sources shown in Table 2). *PFD* pyroclastic flow deposits



to most of the central dome cluster around 0.6–0.5 Ma (Szakács et al. 1993; Pécskay et al. 1995b) (Fig. 13). This stage may have been completed at ca. 0.2 Ma (Pécskay et al. 1995b), the age of the youngest dome lava rocks dated (Table 2). However, because of the age gap between these few samples collected only from loose blocks (Fig. 2) and the rest of the dome rocks, we remain uncertain about the actual age of the most recent dome-building event.

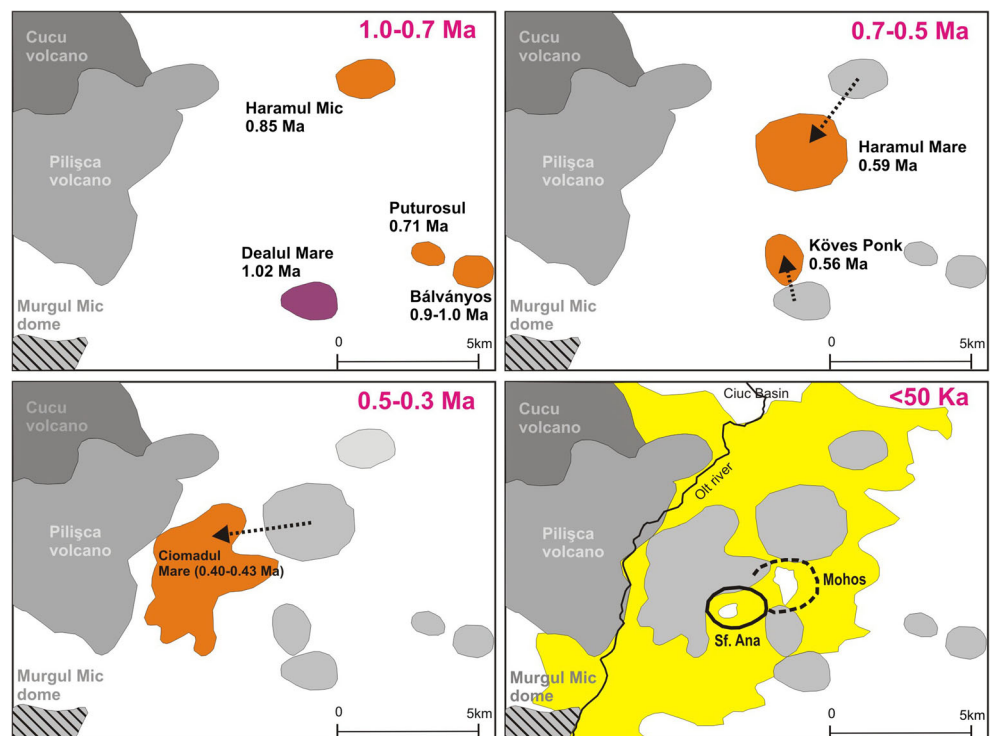
After a period of quiescence of unknown duration, a phreatomagmatic explosive eruption through the Mohoș crater located in the middle of the dome complex generated base-surge deposits and possibly debris flow deposits. The age of this eruption is poorly constrained within the time interval 0.2 Ma to 40 ka. The last eruption occurred at ca. 42–35 ka (Moriya et al. 1996) from the Sf. Ana crater generating the sequence of volcaniclastic deposits found in the south-Tușnad outcrop (Figs. 2 and 6). Due to the explosive nature of both eruptions and the close to undistinguishable composition of their products (Vinkler et al. 2007), the time interval between the two eruptive episodes may be quite short. Moreover, they might well be the two episodes of the same explosive event rather than being two distinct explosive eruptions separated in time by a repose period of the order of tens or hundreds of kiloyears. Supposing that the ca. 40-cm-thick phreatomagmatic deposits in the South-Tușnad sequence (Fig. 6) resulted during the same eruptive episode which generated the Mohoș crater-rim phreatomagmatic deposits and the Mohoș

crater itself, it can be further speculated that the phreatomagmatic event generating the Mohoș crater was a transient episode during the Plinian eruption of Sf. Ana.

Different basement lithologies beneath the two craters (Fig. 2) may explain their contrasting eruptive styles. It is likely that the Barremian-Albian siliciclastic formations beneath the Mohoș crater accumulated larger volumes of groundwater than the more carbonate-rich Tithonic-Neocomian ones beneath the Sf. Ana crater. Magmas coming along the fault zone may have been interacted explosively with near-surface phreatic aquifers (e.g., Morrissey et al. 2000; White and Houghton 2000) in the early phase, while the next phase related to the Sf. Ana crater generated the (sub)Plinian deposits.

Considering the volume of volcanic products building up the dome complex-dominated edifice and the age range of volcanic activity, Ciomadul can be characterized as a very low eruptive frequency volcano. A total volume of ca. 9 km³ of volcanic products currently occur at the surface (Table 4) emplaced over ca. 1 Myr, meaning a minimum output rate of 9 km³/Myr. This is an extremely low value as compared with the CGH output rates (e.g., 143 km³/Myr in the Gurghiu segment, and 109 km³/Myr in the North Harghita segment) and with the average South Harghita segment output rate (39 km³/Myr), but it is consistent with the regional trend of gradually decreasing eruptive rates along the East Carpathian Neogene Volcanic range from NW to SE (Szakács et al. 1997). Similarly, very low (or even lower) output rates can be

Fig. 13 Sketch of the time-space evolution of Ciomadul volcano shown as rock bodies (colored) emplaced in the time intervals of 1.0–0.7 Ma, 0.7–0.5 Ma, 0.5–0.3 kyr and <50 kyr, respectively. Violet (andesite) and orange (dacite) show dome rock composition, and yellow stands for volcaniclastic rocks. Extinct volcanic features are shown in gray tones. Arrows show the direction of shift of volcanic activity from the previous phase



inferred for the Pleistocene rhyolite dome complex of the Coso volcanic field (California, USA) where ca. 1.6 km³ of magma was extruded forming 38 steep-sided domes during a period of ca. 1.2 Myr (Wohletz and Heiken 1992 and Fig. 5.21 within). In that case, however, rhyolitic dome-building activity was accompanied by coeval basaltic volcanism, absent in the Ciomadul area.

Although the K–Ar ages do not seem to be obviously clustered (Fig. 11), one may suppose that this magma output resulted from a small number of eruptive stages (or active periods) in the volcano's history, separated by larger repose-time intervals (in the order of 10⁵ years), rather than from a larger number of active periods separated by shorter repose times (in the order of 10⁴ years). A statistical analysis using the ISOPLOT software (Ludwig 2008) shows four frequency maxima of the K–Ar age distribution—at 0.2, 0.4, 0.6, and 1.0 Ma, respectively—suggesting the likely timing of major dome-building stages at Ciomadul. The repose-time periods between the eruptions are not necessarily of the same duration. The spatial distribution pattern of the dome clusters (Fig. 2) reinforces such an interpretation. On the basis of these considerations, we sketched the eruptive history of Ciomadul (Fig. 13) consistent with all available radiometric age data.

Future activity?

According to the available radiometric age data, Ciomadul volcano is one of the lowest-frequency volcanoes known, with repose-time periods of the order of 10⁴ to 10⁵ years between major active stages. As shown previously (e.g., Szakács et al. 2002; Szakács and Seghedi 2013), it is reasonable to consider the issue of its present activity status and its capability of future eruptions.

Long dormant periods at active volcanoes are known worldwide. Ontake volcano (Japan), for instance, erupted in 1979 after ca. 23 kyr of dormancy (Sano et al. 1998). There are relevant examples in the geological record as well. The much smaller (than Ciomadul) Baruth volcano in the Oligocene Lusatian Volcanic Field, Eastern Germany, for example, shows three stages of evolution in the 27–33-Ma age interval, with repose intervals of ca. 3 Ma between the stages (Tietz et al. 2011). The small-volume (ca. 1.6 km³) rhyolite dome-forming volcanic activity in the Coso volcanic field which lasted for a 1-Myr age interval, and where future eruptions cannot be ruled out (Wohletz and Heiken 1992), is another possible analogy for the Ciomadul case.

Although the precise age of the most recent Plinian/Subplinian eruption from the Sf. Ana crater is still controversial, all available data (Juvigné et al. 1994; Moriya et al. 1996; Vinkler et al. 2007; Harangi et al. 2010) point to a very recent eruption time, on the order of a few tens of kiloyears (10.7–35 kyr) (Table 3; Fig. 12). A number of features and data suggest that at least one crustal magma chamber beneath

Ciomadul is partially molten (Szakács et al. 2002; Szakács and Seghedi 2013). Most probably, the magma chamber is still warm, containing some incompletely solidified magma. However, the capability of the volcanic system of producing further eruptions is more dependent on the state of the deeper magma generation region. The occurrence of subcrustal seismic activity down to ca. 70 km in the vicinity of a “soft” lithosphere column (Popa et al. 2012) might suggest that even the magma generation region and its connection to the crustal magma chamber are not completely frozen and inactive. According to the presently available data, its active status cannot be ruled out completely, and Ciomadul can be viewed as a potentially active volcano. Therefore, future volcanic activity can also be envisaged, but no scientifically sound prediction on the timing of such possible processes can yet be made.

Conclusions

Ciomadul is a small-sized (8.74 km³ in volume) dacite dome-complex volcano. Its main edifice consists of two larger dome clusters and a smaller isolated dome surrounded by volcanoclastic deposits originating from two craters (Mohoš and Sf. Ana) (Fig. 2). Four older satellite domes are located at the northern, southern, and eastern peripheries of, and disconnected from, the main edifice (Fig. 2).

The volcanic evolution of Ciomadul encompasses a ca. 1 Myr time interval (1 ≤ 0.1 Ma). Extrusion of viscous dacite lavas started at ca. 1 Ma generating the peripheral Bálványos and Dealul Mare domes, then shifted to a northern peripheral location at 0.85 Ma (Haramul Mic) and again to an eastern location at 0.7 Ma (Puturosul). The central dome clusters were generated during a much shorter and more intense phase of volcanic activity, between 0.4 and 0.6 Ma. Dome-building activity might have resumed during one more episode at ca. 0.2 Ma. The presence of bread-crusting bombs and blocks among dome rock fragments in debris flow deposits suggests that an explosive event(s) might have punctuated dome formation at as yet unknown eruption center(s). After a significant time gap to account for development of a paleosol (likely 10 s to 120 kyr), two late-phase explosive episodes ended the volcanic activity: one phreatomagmatic from the Mohoš crater, another Plinian/subPlinian from the Sf. Ana crater. The age of the most recent eruption of Ciomadul is loosely constrained by radiocarbon dating of (1) charcoal found in the upper depositional unit of the pyroclastic flow deposits (Juvigné et al. 1994; Moriya et al. 1995, 1996; Harangi et al. 2010), (2) organic matter in the paleosol underlying the Plinian pumice fall deposit (Moriya et al. 1996), and (3) organic material of the Mohoš peat and Sf. Ana lake bottom sediments (Buczko and Magyari 2007; Magyari et al. 2009),

as summarized in Table 2 and Fig. 12. Considering all these data, it is most likely that the Sf. Ana eruption occurred sometime in the 27–35-kyr interval. The age of the older Mohoş eruption is poorly constrained because of the lack of adequate material to be dated by means of radiometric techniques. We speculate that this eruption could have been triggered in close temporal connection with the Sf. Ana one. The reason for the different explosive behavior at the two vents could be the different lithology and hydrogeological behavior of the basement rocks beneath them.

The age data combined with volume calculations show that Ciomadul is a very low frequency volcano with an estimated output rate of $9 \text{ km}^3/\text{Myr}$. This figure, along with the very young age of its last eruption (27–35 ka) and a number of features showing ongoing geodynamic processes in the area (Szakács et al. 2002; Popa et al. 2012; Szakács and Seghedi 2013), suggest the potential for future activity in this region. Although no definite conclusion can be made at this stage, reactivation of the magma generating system and consequent influx of fresh magma into the still incompletely frozen magma chamber beneath Ciomadul remains possible.

Acknowledgments This work was supported by a grant of the Ministry of National Education, CNCS—UEFISCDI, project number PN-II-ID-PCE-2012-4-0137. Field sampling and analytical work of K/Ar dating was supported by, and performed within the framework of bilateral cooperation agreement between the Romanian Academy and the Hungarian Academy of Science. The thoughtful comments and suggestions of improvement from reviewers Daisuke Miura, Andrew Calvert, and Paul Wallace are highly appreciated. We thank Norman Snelling for revision of the English. Răzvan-Gabriel Popa is thanked for his help in a previous version of Fig. 2.

References

- Balogh K (1985) K/Ar dating of Neogene volcanic activity in Hungary: experimental technique, experiences and methods of chronologic studies. *ATOMKI Rep. D/1*, p. 277–288
- Bányai J (1917) The land of Kézdivásárhely, Háromszék county (in Hungarian) Kézdivásárhely vidéke Háromszék vármegyében. *Földtani Közlöny XLVII*, 1–20, Budapest.
- Bányai J (1964) The age of the eruption of the Szent Anna lake twin craters (in Hungarian) A Szent Anna-tavi ikerkráter erupciójának kora. *Földrajzi Értesítő*, XIII, 1, 57–66, Budapest
- Buczko K, Magyari E (2007) The holocene diatom flora of lake Saint Anna (eastern Carpathians, Europe)—archiv für hydrobiologie. *Algol Stud* 124:1–28
- Buczko K, Wojtal A (2007) A new *Kobayasiella* species (Bacillariophyceae) from Lake Saint Anna's sub-recent deposits in Eastern Carpathian Mountains, Europe. *Nova Hedwigia* 84:155–166
- Cassignol C, Gillot PY (1982) Range and effectiveness of unspiked potassium-argon dating: experimental groundwork and applications. In: Odin GS (ed) Numerical dating in stratigraphy. Wiley, Chichester, pp 159–179
- Casta L (1980) Les formations quaternaires de la Dépression de Braşov (Roumanie). PhD Thesis, Université de Aix-Marseille II, 256pp
- Cholnoky J (1922) Some features of the geographic image of the Transylvanian basin. III. Hargita. (in Hungarian) *Földrajzi Közlemények*, 50, 2, 107–122
- Clarke AB, Stephens S, Teasdale R, Sparks RSJ, Diller K (2007) Petrologic constraints on the decompression history of magma prior to vulcanian explosions at the Soufriere Hills volcano, Montserrat. *J Volcanol Geotherm Res* 161:261–274
- Croweller HS, Baneet A, Brown SK, Cottrell E, Deligne NI, Ortiz Guerrero N, Hobbs L, Kiyosugi K, Laughlin C, Lowndes J, Nayembil M, Siebert L, Sparks RSJ, Takarada S, Venzke E (2012) Global database on large magnitude explosive volcanic eruptions (LaMEVE). *J Appl Volcanol* 1:4. doi:10.1186/2191-5040-1-4
- Fink JH, Anderson SW (2000) Lava domes and culees. In H. Sigurdsson et al., eds. *Encyclopedia of volcanoes*. Academic Press, Elsevier, 307–319
- Gillot P-Y (1984) Datation par la méthode du potassium-argon des roches volcaniques récentes (pleistocènes et holocènes). Contributions à l'étude chronostratigraphique et magmatique des provinces volcaniques de Campanie, des Iles Eoliennes, de Pantelleria (Italie du Sud) et de la Réunion (Océan Indien). Thèse, Paris XI-Orsay, 225 pp
- Harangi SZ, Lenkey L (2007) Genesis of the Neogene to Quaternary volcanism in the Carpathian-Pannonian region: role of subduction, extension, and mantle plume. *Geol Soc Am Spec Pap* 418:67–90
- Harangi S, Molnár M, Vinkler AP, Kiss B, Tull AJT, Leonard AG (2010) Radiocarbon dating of the last volcanic eruptions of Ciomadul volcano, Southeast Carpathians, Eastern-central Europe. *Radiocarbon* 52(2–3):1498–1507
- Juvigné E, Gewalt M, Gilot E, Hurtgen C, Seghedi I, Szakács A, Gábris Gy, Hadnagy Á, Horváth E (1994) Une eruption vieille d'environ 10,700 ans (14C) dans les Carpates Orientales (Roumanie). *C.R. Acad. Sci. Paris*, 318, II, 1233–1238, Paris
- Karátson D (2007) From Börzsöny to Hargita. *Volcanology, morphological evolution, paleogeography*. (in Hungarian) Typotex, Budapest, pp. 463
- Karátson D, Timár G (2005) Comparative volumetric calculations of two segments of the Neogene/Quaternary volcanic chain using SRTM elevation data: implications for erosion and magma output rates. *Z Geomorphol Suppl* 140:19–35
- Karátson D, Telbisz T, Harangi S, Magyari E, Dunkl I, Kiss B, Jánosi C, Veres D, Braun M, Fodor E, Biró T, Kósik S, von Eynatten H, Lin D (2013) Morphometrical and geochronological constraints on the youngest eruptive activity in East-Central Europe at the Ciomadul (Csomád) lava dome complex, East Carpathians. *J Volcanol Geotherm Res* 255:43–56
- Krummenacher D (1970) Isotopic composition of argon in modern surface volcanic rocks. *Earth Planet Sci Lett* 8:109–117
- Lexa J, Seghedi I, Németh K, Szakács A, Konecný V, Pécskay Z, Fülöp A, Kovacs M (2010) Neogene-quaternary volcanic forms in the Carpathian-Pannonian region: a review. *Central European Journal of Geosciences* 2, “New advances of understanding physical volcanology processes in the Carpathian-Balkan Region from a global perspective”, 207–270, DOI:10.2478/v10085-010-0025-4
- Lippolt HJ, Mertz DF, Huck K-H (1986) The genesis of the Clara and Friedrich-Christian vein deposits/Central Schwarzwald (FRG): evidence from Rb-Sr, $^{87}\text{Sr}/^{86}\text{Sr}$, K-Arg and $^{40}\text{Ar}/^{39}\text{Ar}$ investigations. *Terra Cognita* 6:228
- Ludwig KR (2008) *Isoplot 3.37*. A geochronological toolkit for Microsoft Excel. Berkeley Geochronology Center Special Publication No. 4
- Luhr JL (2002) Petrology and geochemistry of the 1991 and 1998–1999 lava flows from Volcan de Colima, Mexico: implications for the end of the current eruptive cycle. *J Volcanol Geotherm Res* 117:169–194
- Magyari E, Buczko K, Jakab G, Braun M, Szántó Z, Molnár M, Pál Z, Karátson D (2006) Holocene palaeohydrology and environmental history in the South Harghita Mountains, Romania. *Földtani Közlöny* 136, 2, 249–284, Budapest

- Magyari E, Buczkó K, Jakab G, Braun M, Pál Z, Karátson DM, Pap I (2009) Palaeolimnology of the last crater lake in the Eastern Carpathian Mountains: a multiproxy study of Holocene hydrological changes. *Hydrobiologia* 631:29–63. doi:10.1007/s10750-009-9801-1
- Mason P, Downes H, Thirlwall MF, Seghedi I, Szakács A, Lowry D, Matthey D (1996) Crustal assimilation as a major petrogenetic process in the East Carpathian Neogene and Quaternary continental margin arc. *Rom J Petrol* 37:927–959
- Mason PRD, Seghedi I, Szakács A, Downes H (1998) Magmatic constraints on geodynamic models of subduction in the Eastern Carpathians, Romania. *Tectonophysics* 297:157–176
- Maţenco L, Bertotti G (2000) Tertiary tectonic evolution of the external East Carpathians (Romania). *Tectonophysics* 316:255–286
- Maţenco L, Bertotti G, Leever K, Cloetingh S, Schmid SM, Tărăpoancă M, Dinu C (2007) Large-scale deformation in a locked collisional boundary: interplay between subsidence and uplift, intraplate stress, and inherited lithospheric structure in the late stage of the SE Carpathians evolution. *Tectonics* 26: Art. No. TC4011. DOI: 10.1029/2006TC001951
- Moriya I, Okuno M, Nakamura T, Szakács A, Seghedi I (1995) Last eruption and its ^{14}C age of Ciomadul volcano, Romania (in Japanese with English Abstract). *Summaries of Researches Using AMS at Nagoya University*, VI, 82–91
- Moriya I, Okuno M, Nakamura T, Ono K, Szakács A, Seghedi I (1996) Radiocarbon ages of charcoal fragments from the pumice flow deposit of the last eruption of Ciomadul volcano, Romania (in Japanese with English Abstract). *Summaries of Researches Using AMS at Nagoya University*, VII, 252–255
- Morrissey M, Zimanowski B, Wohletz K, Büttner R (2000) Phreatomagmatic fragmentation. *Encyclopedia of volcanoes*. H. Sigurdsson, B. F. Houghton, S. R. McNutt, H. Rymer and J. Stix. San Diego, USA, Academic Press, 431–445
- Odin GS, Adams CJ, Armstrong RL, Bagdasaryan GP, Baksi AK, Balogh K, Barnes IL, Boelrijk NALM, Bonadonna FP, Bonhomme MG, Cassignol C, Chanin L, Gillot PY, Gledhill A, Govindaraju K, Harakal R, Harre W, Hebeda EH, Hunziker JC, Ingamells CO, Kawashita K, Kiss E, Kreutzer H, Long LE, McDougall I, McDowell F, Mehnert H, Montigny R, Pasteels P, Radicati F, Rex DC, Rundle CC, Savelli C, Sonet J, Welin E, Zimmermann JL, Rundle CC, Savelli C, Sonet J, Welin E, Zimmermann JL (1982) Interlaboratory standards for dating purposes. In: Odin GS (ed) *Numerical dating in stratigraphy*. Wiley, Chichester, pp 123–149
- Panaiotu C, Pécskay Z, Hambach U, Seghedi I, Panaiotu C E, Itaya T., Orleanu M, Szakács A (2004) Short-lived Quaternary volcanism in the Persani Mountains (Romania) revealed by combined K-Ar and paleomagnetic data. *Geol Carpath* 57(4):333–339
- Pécskay Z, Szakács S, Seghedi I, Karátson D (1992) New data on the geochronological interpretation of Cucu volcano and its environs (South Harghita, Romania). (In Hungarian) *Földt. Közl.* 122/2-4, 265–286
- Pécskay Z, Lexa J, Szakács A, Balogh K, Seghedi I, Konečný V, Kovács M, Márton E, Kaličiak M, Széky-Fux V, Póka T, Gyarmati P, Edelstein O, Roşu E, Žec B (1995a) Space and time distribution of Neogene-Quaternary volcanism in the Carpatho-Pannonian Region. *Acta Vulcanol* 7:15–28
- Pécskay Z, Edelstein O, Seghedi I, Szakács A, Kovacs M, Crihan M, Bernad A (1995b) K-Ar datings of the Neogene-Quaternary calc-alkaline volcanic rocks in Romania. In: Downes, H. & Vaselli, O. (eds) *Neogene and related volcanism in the Carpatho-Pannonian Region*. *Acta Vulcanologica* 7:53–63
- Pécskay Z, Lexa J, Szakács A, Seghedi I, Balogh K, Konečný V, Zelenka T, Kovacs M, Póka T, Fülöp A, Márton E, Panaiotu C, Cvetković V (2006) Geochronology of Neogene-Quaternary magmatism in the Carpathian arc and Intra-Carpathian area: a review. *Geol Carpath* 57: 511–530
- Peltz S, Vajdea E, Balogh K, Pécskay Z (1987) Contributions to the chronological study of the volcanic processes in the Calimani and Harghita Mountains (East Carpathians, Romania). *D. S. Inst. Geol. Geofiz.*, 72–73, 1, 323–338, Bucureşti
- Popa M, Radulian M, Szakács A, Seghedi I, Zaharia B (2012) New seismic and tomography data in the southern part of the Harghita Mountains (Romania, Southeastern Carpathians): connection with recent volcanic activity. *Pure Appl Geophys* 169, 9, 1557–1573. doi: 10.1007/s00024-011-0428-6 2010
- Sano Y, Nishio Y, Gamo T, Nagao K (1998) Helium and carbon isotope systematics at Ontake volcano, Japan. *J Geophys Res* 103(B10): 23863–23873
- Scott J (2013) Origin and evolution of the Santiaguito lava dome complex, Guatemala. PhD thesis, Department of Earth Sciences, University of Oxford. 400 pp
- Scott WE, Sherrod DR, Gardner CA (2008) Overview of the 2004 to 2006, and continuing, eruption of Mount Sat. Helens, Washington. *USGS Prof Pap* 1750:3–26
- Seghedi I, Grabari G, Ianc R, Tănăsescu A, Vâjdea E (1986) Rb, Sr, Zr, Th, U, K distribution in the Neogene Volcanics of the South Harghita Mountains. *D.S.Inst.Geol.Geofiz.*,70-71/1, 453–473, Bucharest
- Seghedi I, Szakács A, Udrescu C, Stoian M, Grabari G (1987) Trace element geochemistry of the South Harghita volcanics (East Carpathians). Calc-alkaline and shoshonitic association. *D. S. Inst. Geol. Geofiz.* 72-73/1, 381–397
- Seghedi I, Downes H, Szakács A, Mason PRD, Thirlwall MF, Roşu E, Pécskay Z, Márton E, Panaiotu C (2004) Neogene-Quaternary magmatism and geodynamics in the Carpathian-Pannonian region: a synthesis. *Lithos* 72:117–146
- Seghedi I, Maţenco L, Downes H, Mason PRD, Szakács A, Pécskay Z (2011) Tectonic significance of changes in post-subduction Pliocene–Quaternary magmatism in the south east part of the Carpathian–Pannonian Region. *Tectonophysics* 502:146–157. doi: 10.1016/j.tecto.2009.12.003
- Steiger RH, Jäger E (1977) Subcommittee on geochronology: convention on the use of decay constants in geo- and cosmochronology. *Earth Planet Sci Lett* 36:359–362
- Szakács A, Jánosi CS (1989) Volcanic bombs and blocks in the Harghita Mts. *DS Inst Geol Geofiz* 74(1):181–189
- Szakács A, Seghedi I (1986) Chemical diagnosis of the volcanics from the most southernmost part of the Harghita Mountains—proposal for a new nomenclature. *Rev. Roum. Geol. Geophys. Geogr. GEOLOGIE* 30:41–48, Bucureşti
- Szakács A, Seghedi I (1989) Base surge deposits in the Ciomadul Massif (South Harghita Mts.). *DS Inst Geol Geofiz* 74(1):175–180
- Szakács A, Seghedi I (1995) The Călimani–Gurghiu–Harghita volcanic chain, East Carpathians, Romania: volcanological features. *Acta Vulcanol* 7:145–153
- Szakács A, Seghedi I (1996) Neogene/Quaternary volcanism in Romania. In Seghedi I. (ed.) *Excursion guide A. The 90th Anniversary Conference of the Geological Institute of Romania, June 12–19, 1996, Anuarul Institutului Geologic al României* 69, suppl.2, 33–42, Bucharest
- Szakács A, Seghedi I (2013) The relevance of volcanic hazard in Romania: is there any? *Environ Eng Manag J* 12(1):125–135
- Szakács A, Seghedi I, Pécskay Z (1993) Peculiarities of South Harghita Mts. as terminal segment of the Carpathian Neogene to Quaternary volcanic chain. *Rev Roum de Géol* 37:21–36
- Szakács A, Ioane D, Seghedi I, Rogobete M, Pécskay Z (1997) Rates of migration of volcanic activity and magma output along the Calimani-Gurghiu-Harghita volcanic range, East Carpathians, Romania. *PANCARDI'97, Przglad Geologiczny* 45, 10/2: 1106
- Szakács A, Seghedi I, Pécskay Z (2002) The most recent volcanism in the Carpathian-Pannonian Region. Is there any volcanic hazard?

- Geologica Carpathica, vol. 53. Special Issue, Proceedings of the XVIIth Congress of Carpathian-Balkan Geological Association, 193–194
- Székely A (1959) The geomorphological problematics of the volcanic mountains of Transylvania. (Az erdélyi vulkanikus hegyek geomorfológiai problémái.) (in Hungarian). Földrajzi Közlöny, Budapest
- Tanțău I, Reille M, De Beaulieu JL, Fărcaș S, Goslar T, Paterne M (2003) Vegetation history in the eastern Romanian Carpathians: pollen analysis of two sequences from the Mohoș crater. Veg Hist Archaeobotany 12:113–125
- Teulade A (1989) Téphrologie des formations cendro-ponceuses en milieux lacustres Quaternaires. Méthode et applications au Massif Central français (Velay) et aux Carpathes orientales roumaines (dépression de Brasov). PhD. thesis. Université d'Aix-Marseille II., 298 pp
- Tietz O, Büchner J, Suhr P, Abratis M, Goth K (2011) Die Geologie des Maruther Schafbegers und der Dubrauker Horken—Aufbau and Entwicklung eines känozoischen Vulkancomplexes in Ostsaßen. Berichte der Naturforschenden Gessellschaft der Oberlausitz 18, Supplement, 15–48
- Vance D, Ayres M, Kelley S, Harris NBW (1998) The thermal response of a metamorphic belt to extension: constraints from laser Ar data on metamorphic micas. Earth Planet Sci Lett 162:153–164
- Vinkler AP, Harangi SZ, Ntaflor T, Szakács A (2007) Petrology and geochemistry of pumices from the Ciomadul volcano (Eastern Carpathians)—implication for petrogenetic processes. (in Hungarian with an English abstract). Foldtani Kozlony 137(1): 103–128
- White J, Houghton B (2000) Surtseyan and related phreatomagmatic eruptions. Encyclopedia of Volcanoes. H. Sigurdsson, B. F. Houghton, S. R. McNutt, H. Rymer and J. Stix. San Diego, USA, Academic Press: 495–512
- Wohletz K, Heiken G (1992) Volcanology and geothermal energy. University of California Press, 432 pp
- Wright HMN, Cashman KV, Rosi M, Cioni R (2007) Breadcrust bombs as indicators of Vulcanian eruption dynamics at Guagua Pichincha volcano, Ecuador. Bull Volcanol 69:281–300